Electrostatic Interactions at the Donor Side of the Photosynthetic Reaction Center of Rhodopseudomonas v iridis †

ARTICLE *in* BIOCHEMISTRY · DECEMBER 1998

Impact Factor: 3.02 · DOI: 10.1021/bi980963z · Source: PubMed

Electrostatic Interactions at the Donor Side of the Photosynthetic Reaction Center of *Rhodopseudomonas viridis*†

Frauke Baymann and Fabrice Rappaport*

Institut de Biologie Physico-Chimique, CNRS UPR 1261, 13 rue Pierre et Marie Curie, 75005 Paris, France

Received April 28, 1998; Revised Manuscript Received August 4, 1998

ABSTRACT: The photosynthetic reaction center of *Rhodopseudomonas viridis*, a purple bacterium, contains a tetraheme cytochrome subunit. After its photoinduced oxidation, the primary donor, P, is reduced by the nearby heme (*c*559) of the tetraheme subunit in about 200 ns. This heme, in turn, is reduced by another heme (*c*556) of the subunit in about 2 μs. The midpoint potentials of P, *c*559, and *c*556 are known to be +500, +380, and +320 mV, respectively. The reduction kinetics of P^+ are strongly biphasic in living cells, membrane fragments, and isolated reaction centers. We show here that this biphasicity reflects a small equilibrium constant (lower than 10) for the electron-transfer reaction between P and *c*559, which arises from a significant difference between the operating redox potentials of the P^+/P and *c*559$^+$/*c*559 couples and their equilibrium midpoint potentials. This difference is partly due to the effect of the permanent transmembrane potential, which arises from the cell metabolism, and to significant electrostatic interactions which develop between the electron carriers of the reaction center. Interestingly, the kinetic parameters of P^+ reduction in decoupled cells or membrane fragments are identical to those reported for isolated reaction centers. We estimate an interaction of about 20 mV between *c*556 and *c*559 and about 90 mV between *c*559 and P. Consequently, the operating redox potential of the P^+/P couple is 410 mV.

The reaction center of *Rps. viridis* (Figure 1) is composed of four subunits. Subunits L and M are symmetrically arranged with respect to the membrane normal. They bind a bacteriochlorophyll dimer, P,[1] on the cytoplasmic side of the membrane and a non-heme iron ligated by the two subunits on the periplasmic side of the membrane. Each of the subunits contains a bacteriochlorophyll monomer, a bacteriopheophytin, and a quinone. A menaquinone (Q_A) and a ubiquinone (Q_B) are associated with the L-subunit and M-subunit, respectively. Subunit H and the cytochrome subunit are attached to the reaction center on the periplasmic and on the cytoplasmic side of the membrane, respectively. The cytochrome subunit contains four *c*-hemes that are almost linearly arranged along the protein long axis (*1, 2*). The distance between P and the closest heme is 21 Å (center to center). The hemes are spaced by 14−16 Å (*1*).

The kinetics of the flash-induced electron-transfer reactions and the redox potentials of the cofactors have been studied in detail. After photooxidation of P and reduction of Q_A in the hundreds of picoseconds, P^+ is reduced in about 200 ns by the cytochrome subunit, which is in turn reduced by soluble cytochrome c_2 in the hundreds of microseconds (*3*−*8*). Cytochrome c_2 mediates the electron transfer between the cytochrome bc_1 complex and the reaction center (*7, 9, 10*). The heme closest to P (denoted *c*559 according to its α-band position) has a redox potential of +380 mV. Next are the hemes *c*552, *c*556, and *c*554 with midpoints potentials of +20, +320, and −60 mV, respectively (*4, 11*−*14*).

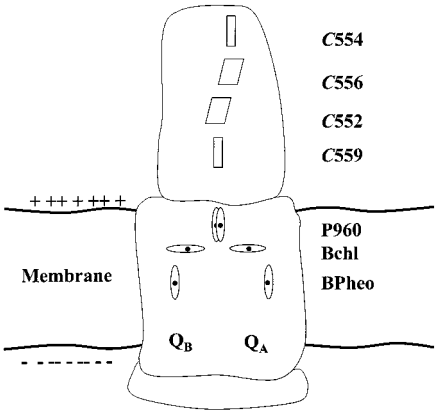

FIGURE 1: Schematic representation of the structure of *Rps. viridis* reaction center and its cofactors.

A careful investigation of the reduction kinetics of P^+ by the tetraheme subunit has shown that it is multiphasic irrespective of the redox state of the tetraheme. Ortega and Mathis have analyzed the reduction kinetics of P^+ by the tetraheme in different redox states and at different temperatures in isolated reaction centers (RC's) (*5*). To account for the multiphasicity of the reduction kinetics of P^+, they proposed kinetically different sub-states of the RC. We have

† This work was supported by the Centre National de la Recherche Scientifique. F.B. is a recipient of a grant from the European Community (ERBFMBICT96707).

* Corresponding author. Email: rappaport@ibpc.fr.

[1] Abbreviations: P^+, oxidized state of the primary donor of the reaction center; *c*556 and *c*559, reduced state of the two high-potential hemes; *c*556$^+$ and *c*559$^+$, oxidized state of the two high-potential hemes; K_{Pc559}, equilibrium constant of the electron-transfer reaction between P and *c*559; ΔG_0, free energy difference of this reaction; FCCP, carbonyl cyanide 4-trifluoromethoxyphenylhydrazone; PMSF, phenylmethylsulfonyl fluoride; PATS3, pyridine-3-carboxaldehydethiosemicarbazone; TMPD, tetramethyl-*p*-phenylenediamine.

10.1021/bi980963z CCC: $15.00
Published on Web 10/16/1998

recently described the flash-induced reduction kinetics of P^+ in whole cells where both the *c*559 and *c*556 hemes are pre-reduced (*8*). Our observations qualitatively agree with those of Ortega and Mathis, since we also observed two distinct phases of P^+ reduction ($t_{1/2}$ 270 ns and 2.4 μs). However, the contribution of the slow component was much larger in whole cells than that reported for RC's (*5*). The relative amplitudes of the 270 ns and 2.4 μs phases in whole cells were 66% and 34%, respectively. For isolated reaction centers, under analogous redox and temperature conditions, Ortega and Mathis reported a 220 ns and a 2 μs component of 85% and 15% relative amplitude, respectively (*5*). To account for the small relative amplitude of the fast phase of P^+ reduction in intact cells, we proposed that the equilibrium constant of this electron-transfer reaction is small [-20 meV, (*8*)]. This would result in a significant amount of P^+ reduced during the microsecond phase, concomitantly with the reduction of oxidized *c*559 by *c*556. However, our calculated equilibrium constant of -20 meV is in strong disagreement with a value of -120 meV derived from the difference in midpoint potentials of the P^+/P and $c559^+/c559$ couples (*4*, *11*). This discrepancy may be rationalized by the transmembrane potential which is generated by the cell metabolism in living bacteria. It is positive on the P-side of the membrane and negative on the Q-side; i.e., its polarity is opposite to the electron transfer of the reaction center. Dracheva et al. (*15*) have shown that the electron-transfer reactions between *c*559 and P^+ and between *c*556 and $c559^+$ are electrogenic. This permanent transmembrane potential is likely to modify the equilibrium constants of the electron-transfer reactions. To test this, we have studied the electron-transfer reactions on the donor site of the RC in the presence or absence of an electrochemical transmembrane potential.

MATERIALS AND METHODS

Cells and Membrane Preparations. Bacteria were grown in Hunter medium in the room light for 24 h and then centrifuged at 4000*g* for 5 min and resuspended in 20 mM TRIS buffer at pH 6.8 for kinetic measurements on whole cells.

For bacterial membrane preparations, 0.2 mM PMSF was added to the suspension buffer as a protease inhibitor. This buffer was used during the entire preparation. Cells were broken in a French press at 16 000 psi and then centrifuged for 20 min at 7700*g*. The supernatant was layered onto a sucrose step gradient with 25 mL of 1.4 M sucrose in the lower phase and 20 mL of 1 M sucrose in the upper phase. Gradients were centrifuged at 55000*g* for 1 h, 30 min, and the membranes were recovered from the interface of the two sucrose concentrations. Membranes were diluted 10-fold, centrifuged for 20 min at 55000*g*, and resuspended in 20 mM TRIS buffer at pH 6.8.

Electrochemical Cell. Redox titrations and kinetic experiments at a fixed potential of +400 mV were performed in an electrochemical cell as described in (*16, 17*). The gold grid was modified with PATS 3. For the kinetic experiments at +400 mV, ferricyanide was used as a redox mediator at a concentration of 50 μM. In the electrochemical redox titrations, a mixture of different mediators was used as described in (*17*).

Inhibitors and Mediators. *o*-Phenanthroline (4 mM) was used as an inhibitor of the Q_A to Q_B electron transfer. In experiments on membrane preparations, TMPD was used to transfer electrons from the cytochrome bc_1 complex to the tetra-heme in the absence of cytochrome *c*.

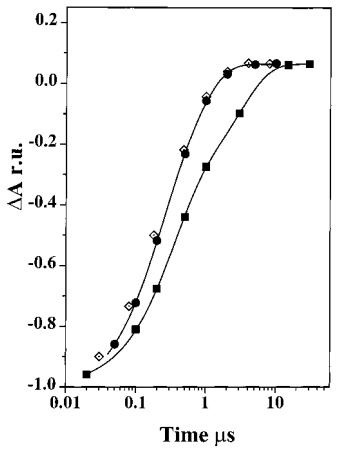

FIGURE 2: Kinetics of P^+ reduction after a flash, in whole cells (squares), whole cells in the presence of 5 μM FCCP (circles), and membrane fragments (open diamonds, in the presence of TMPD). The kinetics have been normalized to their initial amplitudes for better comparison. The lines are the best fits of the data by a sum of two exponentials. The half-times and relative amplitude are as follows: whole cells, 270 ns (66%) and 2.4 μs (34%); in the presence of FCCP, 200 ns (85%) and 2 μs (15%); membrane fragments, 195 ns (86%) and 2 μs (15%).

The ionophore FCCP was used at a concentration of 5 μM in order to disrupt the transmembrane electrochemical potential

Spectrophotometer. Electrochemical titrations on membranes were performed with the spectrophotometer described in (*18*) in the spectrum mode. Kinetic experiments were performed with a home-built spectrophotometer, where the absorption changes are sampled at discrete times by short flashes. These flashes are provided by a Nd:Yag-pumped (355 nm) Optical Parametric Oscillator which produces monochromatic flashes [1 nm full width at half-maximum of 6 ns (fwhm) duration]. Excitation was provided by the fundamental frequency (1064 nm) of a Nd:Yag laser (50 mJ). The technical aspects and characteristics of this spectrophotometer will be described elsewhere

Data Acquisition, Calculation of Equilibrium Constants, Spectra, and Reaction Rates. The kinetics of P^+ reduction were followed at the wavelength pair 610 nm$-$590 nm. The kinetic data were measured at several wavelengths between 540 and 570 nm. They were fitted by a global fit procedure (Levenberg$-$Marquardt algorithm and general linear least-squares algorithm) to obtain the rate constants and spectra of the different kinetic phases. The total amplitude obtained by the fit corresponds to the overall amplitude extrapolated to $t = 0$. The residue of the fit is the remaining absorbance difference between the initial state before flash excitation and the final state, reached after completion of the fitted kinetic phases. The midpoint potentials of the hemes and their corresponding spectra have been obtained by a global fit with the program mE_h-fit (*19*) of the data obtained by electrochemical redox titration.

RESULTS

Whole Cells. Figure 2 shows the kinetics of P^+ reduction under different experimental conditions. As reported in (*8*),

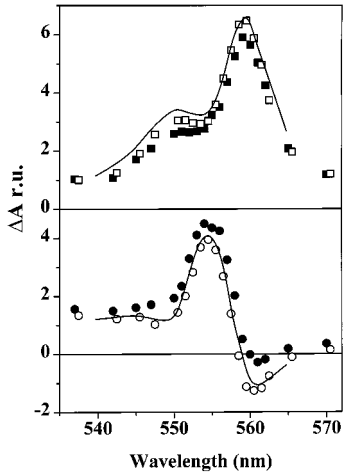

FIGURE 3: Spectra of the submicrosecond (top) and microsecond (bottom) reduction phases in the α-band region of the hemes, calculated by a global fit analysis. Closed symbols, whole cells; open symbols, whole cells in the presence of 5 μM FCCP; lines, membrane fragments. All spectra have been normalized to the same amplitude of P^+ formation after one actinic flash. The half-time of the submicrosecond phase was 270 ns in the absence of FCCP and 200 ns in its presence. The half-time of the microsecond phase was 2.4 μs in the absence and 2 μs in the presence of FCCP.

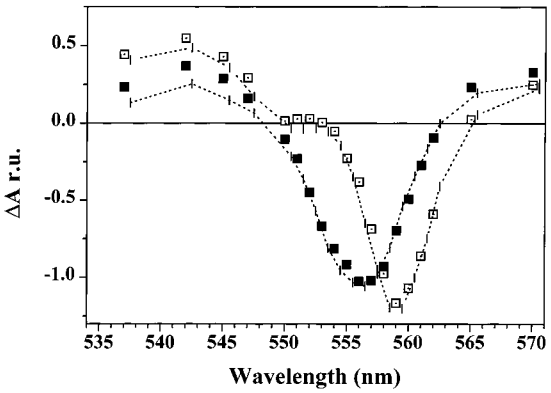

FIGURE 4: Spectra of *c*559 and *c*556 oxidation computed from the kinetic data. The spectra were computed by solving the following equations: (1) $\Delta A^f(\lambda) = \alpha(\Delta\epsilon_P - \Delta\epsilon_{c559})$; (2) $\Delta A^s(\lambda) = (1 - \alpha)(\Delta\epsilon_P - \Delta\epsilon_{c556}) + \alpha(\Delta\epsilon_{c559} - \Delta\epsilon_{c556})$, where $\Delta A^f(\lambda)$ and $\Delta A^s(\lambda)$ stand for the amplitude of the submicrosecond and microsecond phases at wavelength λ, respectively; α stands for the relative amplitude of the submicrosecond phase; and $\Delta\epsilon_P$, $\Delta\epsilon_{c559}$, and $\Delta\epsilon_{c556}$ are the absorbance changes due to P, *c*559, and *c*556 oxidation, respectively. Closed squares, spectrum of *c*559 oxidation; open squares, spectrum of *c*556 oxidation, both in the presence of the permanent $\Delta\tilde{\mu}_H$. Spectra obtained in the absence of the permanent $\Delta\tilde{\mu}_H$ are shown by bars and dotted lines.

*c*559 and *c*556 are reduced before the flash in intact, dark-adapted bacteria. The data could be fitted by a sum of two exponentials. After the flash, 66% of P^+ is reduced with a half-time of 270 ns. The remaining fraction of 34% is reduced with a half-time of 2.4 μs. Thus, in agreement with results obtained with purified RC's (*5*) or membrane fragments (*6*), the kinetics of reduction of P^+ are markedly biphasic. However, the relative amplitude of the slow phase ($t_{1/2} \sim 2$ μs) is about twice as large in whole cells as in isolated RC's or in membrane fragments. To test whether the transmembrane electrochemical potential is responsible for this difference, we added FCCP, a proton carrier, known to disrupt the transmembrane potential. As shown in Figure 2, addition of FCCP induced a significant change of the relative amplitudes of the two phases of P^+. The relative amplitude of the submicrosecond phase was 85%, while that of the microsecond phase was 15%. Interestingly, the rates of both phases increased slightly ($t_{1/2}$ ~200 ns and 2 μs).

Figure 3 shows the spectra of the two kinetic phases in whole cells, in the α-band region of the hemes. The submicrosecond reaction (top panel) displays the spectral features of the oxidation of *c*559 by P^+. Its amplitude is larger in the presence than in the absence of FCCP. Thus, both the amount of oxidized *c*559 and the relative amplitude of the submicrosecond phase of P^+ reduction are larger in the absence of a transmembrane potential. We reported previously (*8*) that the spectrum of the microsecond kinetics in the absence of FCCP shows a positive peak at 555 nm that is much larger than the negative one at 560 nm. This is illustrated in Figure 3 (lower panel). This asymmetric shape indicates that the amount of oxidized *c*556 is larger than the amount of reduced *c*559. We therefore proposed a low equilibrium constant for the electron-transfer reaction between P and *c*559 (*8*). Upon addition of FCCP, the relative amplitude of the submicrosecond phase (the reduction of P^+ by *c*559) increases, which correlates to an increase of the amplitude of the negative peak of the spectrum of the microsecond phase (which is the signature of the reduction of *c*559 by *c*556). Together, these data strongly support the interpretation proposed in (*8*) of a low equilibrium constant (K_{Pc559}) in intact cells resulting from the transmembrane electrochemical potential ($\Delta\tilde{\mu}_H$).

The spectrum of P oxidation may be obtained by extrapolating the absorption changes to $t = 0$ at each wavelength. In the present framework, after appropriate weighting to take into account the relative amplitude differences of the two kinetic phases, the spectra of overall *c*559 and *c*556 oxidation may be computed. Results are shown in Figure 4 for whole cells in the presence and absence of FCCP. The spectra were normalized to the same amplitude of P^+ formation measured 20 ns after the flash at 550 nm. Although the relative amplitudes of the submicrosecond and microsecond phases differed significantly in these two sets of experiments (see Figure 3), the above computation gave identical overall amplitudes for the spectra of *c*559 and *c*556 oxidation, respectively. This shows that the changes in the amount of P^+ reduced during the submicrosecond phase strictly correlated to the changes in the amount of oxidized *c*559 during this phase. These results strongly support the hypothesis of a change in K_{Pc559} induced by the collapse of the permanent $\Delta\tilde{\mu}_H$.

However, even in the absence of a permanent $\Delta\tilde{\mu}_H$ (i.e., in the presence of FCCP), the reduction kinetics of P^+ were still markedly biphasic, and the spectrum of the microsecond phase was still asymmetric. Possibly, the flash-induced transient transmembrane electrical potential influences the electron-transfer reactions. Figure 3 (bottom) shows that the effect of the transmembrane potential on the amplitude of the microsecond phase can be conveniently observed at 561 nm (the negative peak of the difference between the spectra of *c*559 and *c*556 oxidation). We thus measured the amplitude of this phase at 561 nm at different flash intensities (data not shown). As expected, this amplitude decreased with increasing flash intensities (i.e., increasing flash-induced $\Delta\Psi$). Yet, the data presented in Figures 2 and 3 were recorded with a low flash intensity so that the flash-induced $\Delta\Psi$ was unlikely to account for the low value of the

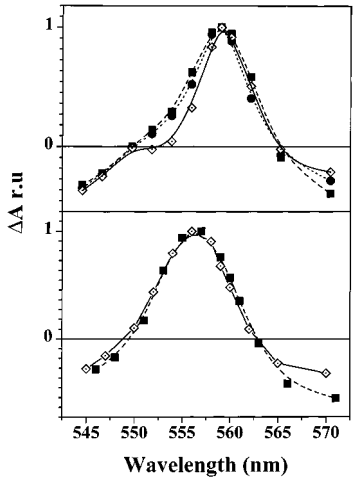

FIGURE 5: Top: spectra of *c*559 reduction obtained by kinetics (see text, open diamonds), electrochemistry (squares), and recombination between Q_A^- and *c*559$^+$ in the presence of 4 mM *o*-phenanthroline (circles). Bottom: spectra of *c*556 reduction obtained by kinetics (see text, open diamonds) and electrochemistry (squares).

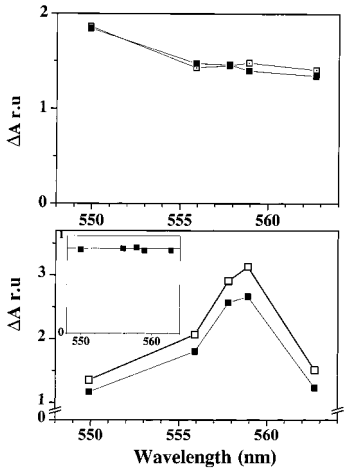

FIGURE 6: Top panel: absorption changes resulting from the oxidation of P^+ measured 20 ns after the first and the second flash (open and closed symbols respectively). Bottom panel: spectra of the submicrosecond phase of P^+ reduction by *c*559 after one (open symbols) and two (closed symbols) flashes, with membranes poised at an external redox potential of 200 mV. The inset shows the ratio between the two spectra of *c*559.

equilibrium constant K_{Pc559} in the absence of $\Delta\tilde{\mu}_H$. To test this, we repeated these experiments with membrane fragments because no photoinduced $\Delta\Psi$ is expected with this material.

Membrane Fragments. In kinetic experiments with membranes, TMPD was used as an electron carrier between the reaction center and the cytochrome bc_1 complex. TMPD has been shown to donate electrons slowly enough not to disturb the electron-transfer chain between *c*556, *c*559, and P. The reduction kinetics of P^+ in these conditions are shown in Figure 2. These data could be fitted by a sum of two exponentials. The fast and slow phases had half-times of 195 ns and 2 μs and accounted for 86% and 14% of the signal, respectively. These values are in good agreement with those of Dohse et al. with membrane fragments (*6*) and those of Ortega and Mathis with purified RC's (*5*). As seen from Figure 2, membrane fragments gave very similar results to those obtained with whole cells in the presence of FCCP.

Electrochemical redox titrations of these membrane fragments showed midpoint potentials of +330 mV for *c*556 and +395 mV for *c*559, or a difference of 65 mV which is in good agreement with values obtained both for isolated RC's and of membrane fragments (*4, 11*). The redox-induced difference spectra of the two hemes, obtained by a fit of the data with a sum of two $n = 1$ Nernst functions, are shown in Figure 5. It is noteworthy that the shoulder at 550 nm in the *c*559 spectrum is much less pronounced when obtained by redox titration than by kinetic experiments.

To investigate the influence of the redox state of *c*556 on the equilibrium constant between P^+ and *c*559, we compared the kinetics of electron transfer between P^+ and *c*559 in the presence of *c*556 oxidized and reduced. In double flash experiments, we adjusted the TMPD concentration so that the slow reduction of the hemes was much slower than the 100 ms time interval between two actinic flashes (not shown). Under these conditions, the second flash is expected to hit those centers in which *c*556 is oxidized by the first flash and has not yet been rereduced by TMPD. After the second flash (i.e., in the presence of oxidized *c*556), the half-time of reduction of P^+ was 245 ns, in good agreement with the value of 230 ns reported in (*5*). Figure 6 shows the spectra of the submicrosecond phase of P^+ reduction after the first and second actinic flashes. These were identical but of different amplitude. The ratio between the two spectra (inset in Figure 6) shows that only 88% of the *c*559 which has been oxidized after the first flash (and subsequently reduced by *c*556) is oxidized after the second flash. This is not due to a smaller yield of charge separation after the second flash because, as shown in Figure 6, the amount of P^+ formed by the two flashes was identical. We thus conclude that the equilibrium constant K_{Pc559} is smaller if *c*556 is oxidized than if it is reduced.

Spectra of P^+ formation, measured 30 ns after a flash or calculated by extrapolation of the amplitude to $t = 0$, were nearly identical and display a maximum around 559 nm (Figure 7). Its line shape suggests that it reflects a P^+-induced electrochromic shift of the α-band of reduced *c*559. To test this, we recorded the oxidation spectrum of P in the presence of oxidized *c*559. To this end, the redox potential was poised at +460 mV in the electrochemical cell. At this potential, *c*556 and most of *c*559 are oxidized before the flash. *o*-Phenanthroline was added to inhibit the Q_A to Q_B electron transfer, thereby allowing charge recombination between P^+ and Q_A^-. The amplitude of the spectrum of P^+ formation (measured 50 ns after the flash) was smaller than that of the spectrum measured in the presence of reduced *c*559, presumably because of a significant fraction of preexisting centers in the P^+ state. Apart from this difference in amplitude, the two spectra were very similar except in the 559 nm region. When *c*559 was oxidized, we no longer detected the 559 nm peak. Because oxidized cytochromes have a very broad α-band with a small extinction coefficient, we interpret the 559 nm feature observed in the presence of reduced *c*559 as an electrochromic shift of the reduced *c*559 α-band superimposed on the oxidation spectrum of P^+.

Similar experiments were performed at an external potential of +400 mV. Under these conditions, most of *c*556 and a part of *c*559 are oxidized before the flash. Charge recombination between P^+ and Q_A^- is expected to occur in

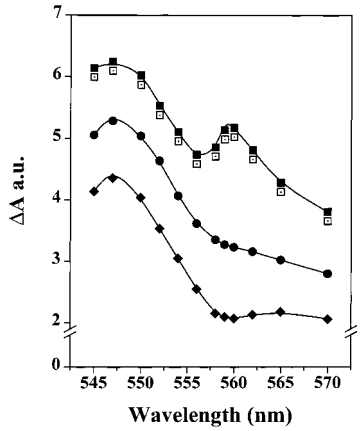

FIGURE 7: Spectra of P oxidation. Upper spectra: extrapolated amplitude at $t = 0$ (closed squares) and absorption changes 30 ns after a flash (open squares) with membrane fragments poised at a redox potential of +200 mV (i.e., in the presence of reduced *c*559). Middle spectrum: absorption changes 50 ns after a flash with membrane fragments poised at a redox potential of 460 mV, i.e., in the presence of *c*559 oxidized (electrochemical cell in the presence of 2 mM *o*-phenanthroline). Lower spectrum: spectrum of the 85 ms charge recombination phase with membrane fragments poised at a redox potential of +400 mV in the presence of 2 mM *o*-phenanthroline. The spectra have been arbitrarily shifted vertically for better comparison.

the fraction of centers containing *c*559 already oxidized. Since formation of Q_A^- does not induce any absorption changes in this wavelength region, the spectrum of this recombination phase should yield the spectrum of P^+ formation in the presence of oxidized *c*559 (Figure 7, bottom). Here again, no bandshift was seen in the 559 nm region.

Charge recombination between Q_A^- and *c*559$^+$ is expected to occur, in the fraction of centers containing prereduced *c*559. The spectrum of this phase should thus yield the spectrum of *c*559 oxidation. This spectrum is shown in Figure 5. It closely resembles the spectrum obtained by redox titrations. In good agreement with the findings of Gao et al. (*20*), the charge recombination reactions between Q_A^- and P^+ took place with a 820 μs half-time, whereas those between Q_A^- and *c*559$^+$ had a half time of 84 ms.

DISCUSSION

Equilibrium Constant. We propose that the biphasic reduction kinetics of P^+ reflect the low equilibrium constant of the electron-transfer reaction between *c*559 and P^+. This equilibrium constant may be estimated by the ratio of the relative amplitude of the fast phase versus that of the slow phase. The results of this calculation and the corresponding free energy differences are summarized in Table 1. They strongly depend on the experimental conditions, i.e., the redox state of the sample and the transmembrane potential. Identical results were obtained from cells in the presence of FCCP, membrane fragments, and isolated reaction centers (*5*), as long as the two high-potential hemes were in the reduced state prior to the flash. In all cases, the equilibrium constants are much smaller than the value of 100 ($\Delta G_0 = -120$ meV) expected from the measured differences in redox potentials of the P^+/P and *c*559$^+$/*c*559 couples.

Our calculation of the equilibrium constants (summarized in Table 1) is valid, provided that the charge equilibration between *c*559 and P and that between *c*556 and *c*559 are well separated in time (i.e., the equilibrium of the electron-transfer reaction between P^+ and *c*559 is reached before the oxidation of *c*556 proceeds). In *R. viridis* reaction centers, the ratio of the half-times of both reactions is about 10, making the above assumption reasonable.

Table 1: Half-Time ($t_{1/2}$), Relative Amplitude, Equilibrium Constant K_{Pc559}, Free Energy ΔG_0, and Rate Constant k_{et} of Electron Transfer between *c*559 and P^+[a]

electron transfer, *c*559 → P^+	cells	cells with FCCP	membranes with reduced *c*556	membranes with oxidized *c*556
obs $t_{1/2}$ (ns)	270	200	195	245
amplitude of sub-μs phase (%)	66	85	86	76
K_{Pc559}	1.95	5.7	6.15	3.2
ΔG_0 (meV)	−17	−45	−47	−30
k_{et} ($\times 10^6$ s^{-1})	1.7	3	3.1	2.3

[a] k_{et} is computed according to the equation: $k_{et} = (\ln 2/t_{1/2}^{obs})(1 + 1/K_{Pc559})$.

The acceleration of the electron-transfer reactions observed upon addition of the uncoupler FCCP to whole cells as well as the effect of flash intensity on the amount of oxidized *c*559 shows that the equilibrium constant K_{Pc559} is strongly sensitive to the transmembrane $\Delta\Psi$. Addition of FCCP, known to disrupt the permanent membrane potential, induced an increase of the equilibrium constant from 1.95 to 5.7. When the actinic flash intensity was increased, K_{Pc559} decreased, confirming the role of a flash-induced membrane potential in addition to the static membrane potential. This may account for the slightly larger equilibrium constant observed with membrane fragments in which charge redistribution should immediately eliminate the flash-induced potential. Experiments with other species have shown that even in the presence of FCCP the flash-induced membrane potential lasts for several tens of milliseconds, which is much longer than the time needed for completion of the electron-transfer reactions (*Rhodobacter sphaeroides*, for example, allows monitoring of changes in its membrane potential by shifts in carotenoid absorption bands).

The electron-transfer reactions between *c*559 and P^+ and between *c*556 and *c*559$^+$ are both affected by the transmembrane potential. This shows that the effect of the latter is not restricted to the intramembrane region but extends within the tetraheme into the bulk phase. Dracheva et al. (*15*) came to the same conclusion, reporting that the electron transfer from *c*556 to *c*559 is responsible for 5% of the electrogenicity induced by the charge separation between *c*556 and Q_A^-. The transmembrane potential is positive on the donor side of the membrane and is thus expected to shift the redox potentials of the cofactors at this side of the membrane to higher values. The equilibrium constant of the electron-transfer reaction between P and *c*559 is decreased by the presence of a transmembrane potential. We therefore conclude that the transmembrane $\Delta\tilde{\mu}_H$ induces a larger increase of the redox potential of *c*559 than of P and that the difference between the two midpoint potentials decreases.

Electrostatic Interactions. The effect of the transmembrane potential alone is insufficient to account for the discrepancy between the values of K_{Pc559} reported here and the value of 100 expected from the difference in midpoint potentials of the *c*559$^+$/*c*559 and of the P^+/P couples. In

uncoupled whole cells as well in membrane fragments, we estimate K_{Pc559} to be about 6 ($\Delta G_0 \approx -45$ meV). We conclude that significant electrostatic interactions between the cofactors account for this apparent discrepancy. With membrane fragments, an equilibrium constant of 6.15 ($\Delta G_0 = -47$ meV) is observed for the reaction between P^+ and *c*559 after one flash, in the presence of reduced *c*556. After the second flash, this reaction occurs in the presence of oxidized *c*556. This results in a lower yield for the oxidation of *c*559. We estimate the equilibrium constant in this case to be 3.2 ($\Delta G_0 = -30$ meV). The difference in free energy for the reduction of P^+ by *c*559 is therefore lower by 17 mV (17 mV = 47 − 30 mV). Assuming that the redox state of *c*556 has no influence on the potential of P, this 17 mV difference would reflect the electrostatic interaction between *c*556 and *c*559. This estimate confirms the electrostatic interaction of 14 mV calculated by Gunner and Honig (*21*).

The spectra of the different electron carriers further reflect these electrostatic interactions. Figure 5 shows the spectra of *c*559 oxidation as obtained by kinetics, recombination experiments, and redox titrations. In the spectra calculated from electrochemical titrations or obtained by charge recombination between Q_A^- and $c559^+$, the shoulder observed around 550 nm is significantly less pronounced than in the spectrum computed from the submicrosecond phase of P^+ reduction. This difference may be explained by a small contribution of the *c*556 oxidation spectrum to the former spectra. We propose that this contribution arises from the relatively close values of the midpoint potentials of the two hemes combined with an electrostatic interaction between these hemes. Because of the latter, the midpoint potential of each heme is dependent on the redox state of its counterpart. Thus, the difference in midpoint potentials of the two hemes varies as the redox states are titrated. As an example, the midpoint potential of *c*559 is expected to increase as *c*556 is oxidized. Consequently, fitting the data with a sum of two Nernst functions would not completely separate the spectra of the two hemes. A small contribution of the spectrum of *c*556 oxidation (and conversely, the spectrum of *c*559 oxidation) should be superimposed to the spectrum of *c*559 (conversely the spectrum of *c*556 oxidation). In charge recombination experiments, *c*556 is mostly oxidized prior to the flash, and the distribution of the reducing equivalent is determined by the redox equilibria between the different electron carriers. The flash-induced oxidation of c559 should result in an increase of the amount of oxidized *c*556. Since the redox equilibrium between the two hemes is achieved in the microsecond time range whereas the charge recombination reaction proceeds in the 100 ms time range, the reducing equivalent is redistributed during charge recombination so that a small reduction of $c556^+$ is superimposed on the reduction of $c559^+$

We assume that the redox potential of *c*556 is the same in equilibrium redox titrations and in kinetic experiments, because in both cases the redox changes of this heme occur in the presence of reduced *c*559 and P. The midpoint potential of *c*559 obtained in equilibrium redox titrations, however, takes into account the electrostatic interaction between the two hemes. We thus propose that in the presence of reduced *c*556 the midpoint potential of *c*559 would be about 360 mV (385 − 17 mV = 358 mV). Our

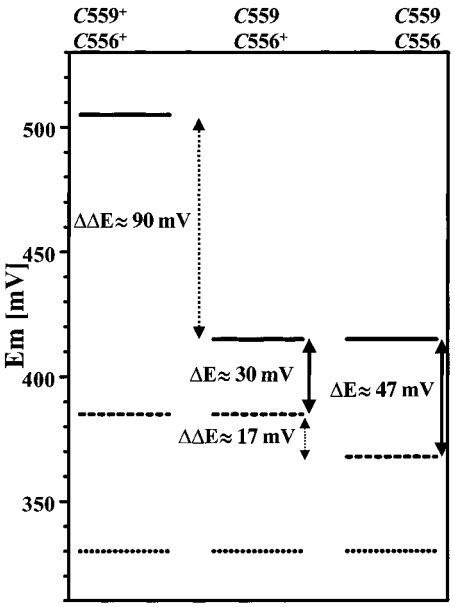

FIGURE 8: Redox potentials of the different cofactors and the electrostatic interactions between them under various redox conditions (solid lines, dashed lines, and dotted lines: redox potentials of P, *c*559, and *c*556, respectively). The presence of the reduced form of the hemes in the tetra-heme subunit lowers the redox potential of P and accounts for the small equilibrium constant between P^+ and *c*559. The influence of Q_A^- on the redox potentials of P and the hemes has not been taken into consideration.

data show that the free energy difference between *c*559 and P is about 50 mV in isolated membranes. Consequently, the operating redox potential of P is +410 mV (360 + 50 mV = 410 mV). The difference between this value and the redox potential of +500 mV, determined by equilibrium redox titrations, yields an electrostatic interaction of 90 mV between *c*559 and P. Figure 8 summarizes these considerations. For these calculations, we assumed that the electrostatic interaction between Q_A and P is negligible. If this were otherwise, the presence of a charge on Q_A would probably lower the redox potential of P more than that of *c*559. The value of 90 mV therefore represents an upper limit for the interaction between the two cofactors.

The existence of an electrostatic interaction between P and *c*559 is further supported by the electrochromic shift of the α-band of *c*559 induced by the oxidation of P as discussed above (Figure 7).

The *c*559 heme and P are separated by 21 Å center-to-center in the protein. The *c*559 and *c*556 hemes are spaced by 24 Å (*1*). The interaction is smaller between the two hemes than between P and *c*559. This reflects the larger distance from the membrane plane (i.e., their location in a part of the protein where the dielectric constant is presumably larger). This is consistent with the findings of Dracheva et al. (*15*) of a larger electrogenicity associated with the reduction of P^+ by *c*559 than with the reduction of $c559^+$ by *c*556 (15% and 5%, respectively). Furthermore, *c*554 is located between *c*556 and *c*559 (*11*−*14*) and may increase the dielectric constant in this region of the protein.

In principle, it is possible to derive the values of the equilibrium constant, and thus of the electrostatic interaction between electron carriers, from recombination experiments. The recombination rate $k_r^{c559Q_A}$ between *c*559 and Q_A^- is given by the following equation:

$$k_r^{c559Q_A} = k_r^{PQ_A}(1 + K_{Pc559})^{-1}$$

where $k_r^{PQ_A}$ is the rate of the charge recombination reaction between P^+ and Q_A^- in the presence of reduced *c*559.

This rate is unfortunately not accessible experimentally since the reduced *c*559 heme is expected to reduce P^+ much faster than Q_A^- reduces P^+. We have measured the rate constant of recombination between Q_A^- and *c*559$^+$ to be 8.3 s^{-1}, in good agreement with (*20*). From the above equation and our estimation of K_{Pc559}, we computed the rate of the charge recombination reaction between P^+ and Q_A^- in the presence of reduced *c*559 to be 58 s^{-1}. This value is more than 1 order of magnitude smaller than the 840 s^{-1} rate constant of recombination between Q_A^- and P^+ measured in the presence of oxidized *c559* (*20* and the present paper). These data suggest a strong dependence of the rate of the charge recombination reaction between P^+ and Q_A^- on the redox state of *c*559. The present data therefore strongly support the existence of an electrostatic interaction between P and *c*559. The oxidation of the former induces an α-band-shift of the latter since the midpoint potential of the P^+/P couple is dependent on the redox state of *c*559. The electrostatic interaction most likely modulates the charge recombination reaction. Recent studies of Lin et al. have shown substantial effects of the redox potential of the P^+/P couple on the rate of recombination between P^+ and Q_A^- in *Rhodobacter sphaeroides* (*22*). In addition, the rate of the electron-transfer reactions between P^+ and *c*559 depends significantly on the redox state of the tetraheme subunit (*5*, *8*, *15* and the present paper).

ACKNOWLEDGMENT

Ongoing and stimulating discussions with P. Joliot, J. Lavergne, O. Vallon, and A. Verméglio are gratefully acknowledged. F.-A. Wollman and T. Kallas are acknowledged for critical reading of the manuscript.

REFERENCES

1. Deisenhofer, J., Epp, O., Miki, K., Huber, R., and Michel, H. (1985) *Nature 318*, 618−6242.
2. Nitschke, W., and Dracheva, S. M. (1995) in *Anoxygenic Photosynthetic Bacteria* (Blankenship, R. E., Madigan, M. T., and Bauer, C. E., (Eds.) pp 775−805, Kluwer Academic Publishers, Dordrecht, The Netherlands.
3. Shopes, R. J., Levine, L. M. A., Holten, D., and Wraight, C. A. (1987) *Photosynth. Res. 12*, 165−180.
4. Dracheva, S. M., Drachev, L. A., Zaberezhnaya, S. M., Konstantinov, A. A., Semenov, A. Y., and Skulachev, V. P. (1986) *FEBS Lett. 205*, 41−46.
5. Ortega, J. M., and Mathis, P. (1993) *Biochemistry 32*, 1141−1151.
6. Dohse, B., Mathis, P., Wachtveitl, J., Laussermair, E., Iwata, S., Michel, H., and Oesterhelt, D. (1995) *Biochemistry 34*, 11335−11343.
7. Garcia, D., Richaud, P., and Verméglio, A. (1993) *Biochim. Biophys. Acta 1144*, 295−301.
8. Rappaport, F., Béal, D., Verméglio, A., & Joliot, P. (1998) *Photosynth. Res.* (in press).
9. Shill, D. A., and Wood, P. M. (1984) *Biochim. Biophys. Acta 764*, 1−7.
10. Knaff, D. B., Willie, A., Long, J. E., Kriauciunas, A., Durham, B., and Millett, F. (1991) *Biochemistry 30*, 1303−1310.
11. Fritzsch, G., Buchanan, S., and Michel, H. (1989) *Biochim. Biophys. Acta 977*, 157−162.
12. Nitschke, W., and Rutherford, A. W. (1989) *Biochemistry 28*, 3161−3168.
13. Verméglio, A., Richaud, P., and Breton, J. (1989) *FEBS Lett. 243*, 259−263.
14. Alegria, G., and Dutton, P. L. (1991) *Biochim. Biophys. Acta 1057*, 258−1972.
15. Dracheva, S. M., Drachev, L. A., Konstantinov, A. A., Semenov, A. Y., Skulachev, V. P., Arutjunjan, A. M., Shuvalov, V. A., and Zaberezhnaya, S. M. (1988) *Eur. J. Biochem. 171*, 253−264.
16. Moss, D. A., Nabedryk, E., Breton, J., and Mäntele, W. (1990) *Eur. J. Biochem. 187*, 565−572.
17. Baymann, F., Moss, D. A., and Mäntele, W. (1991) *Anal. Biochem. 199*, 269−274.
18. Joliot, P., Beal, D., and Frilley, B. (1980) *J. Chim. Phys. 77*, 209−216.
19. Grzybek, S., Baymann, F., Müller, K.-H., & Mäntele, W. (1993) in *Fifth international conference on the spectroscopy of biological molecules* (Theophanides, T., Anastassopoulou, J., and Fotopoulos, N., Eds.) pp 25−26, Kluwer Academic Publishers, Dordrecht.
20. Gao, J.-L., Shopes, R. J., and Wraight, C. A. (1990) *Biochim. Biophys. Acta 1015*, 96−108.
21. Gunner, M. R., and Honig, B. (1991) *Proc. Natl. Acad. Sci. U.S.A. 88*, 9151−9155.
22. Lin, X., Murchison, H. A., Nagarajan, V., Parson, W. W., Allen, J. P., and Williams, J. C. (1994) *Proc. Natl. Acad. Sci. U.S.A. 91*, 10265−10269.

BI980963Z